

Computer simulation and infrared investigation on a novolac formaldehyde phenolic resin

B. L. SCHÜRMAN*, L. VOGEL

Federal Institute of Materials Research and Testing (BAM), Unter den Eichen 87, D-12203 Berlin, Germany

Atomistic molecular dynamics computer simulations and infrared experiments have been performed to characterize the solid state of a formaldehyde phenolic resin. The infrared measurement of Novolak 1940H qualitatively proves the existence of hydrogen bonding. Upon heating, the band of the free O–H vibrations increased at the cost of the associated band. The simulation of a system of purely ortho-substituted chains in comparison to the ensemble of randomly ortho–para substituted chains, showed that the amount of hydrogen bonding, which in both cases mainly acts intramolecularly, is much smaller in the latter system due to the larger separation of the polar OH groups.

1. Introduction

Polymeric materials built of amorphous structures are of great interest in a variety of applications. When polymer chains are cooled down from the melt they can form an amorphous structure possessing surprisingly good mechanical and thermal properties. Because of the complexity and lack of order in these structures, their characteristic parameters are not accessible by the techniques used for the characterization of crystalline polymers. The detailed structure and dynamics which define mechanical and thermal properties are difficult to obtain by the presently available experimental methods. Usually, scattering methods provide global chain dimensions such as the radius of gyration and end-to-end distance or density.

Another complementary way to overcome this lack of data is to build amorphous structures with an algorithm developed and tested by Suter and co-workers [1–4] and to perform molecular dynamics (MD) computer simulations on the basis of these ensembles in order to analyse the trajectories with respect to physical properties.

Our specific interest in this study was focused on modelling of a novolac formaldehyde phenolic resin. Adding a hardener to this compound creates a network called duroplast, which is widely used in electrical and appliance products as well as in high-technology materials. Phenolic resins have a comparatively long history: commercial production started in 1907 [5] and the publications dealing with chemical analytical aspects of different phenolic compounds go back to the sixties [6, 7]. Our Institute is involved in the quality control of phenolic moulding powders and in exploring this material down to the

microscopic level. Meanwhile, it is known [8] and repeatedly proven [9] that the glass transition temperature is comparatively high (57°C); dielectric measurements [9] on industrial novolak indicate, through interpretation of the ϵ'' master curve, strong inter- and intramolecular interactions, but because these parameters are extracted from a fitting procedure of a global property, very little is really known about the motion on the molecular level, and quantitative statements about the character of the interactions have not been made. In this study, a model of the amorphous structure was generated and physical properties, such as characteristic ratio, X-ray diffraction pattern and radial distribution function, were calculated. In particular, the role of hydrogen bonding was investigated.

2. Model and simulation

As the starting structure we used the repeat unit displayed in Fig. 1 with a degree of polymerization of $n = 15$ in ortho–ortho sequence and a methyl terminator at one chain end, so that one single chain consists of 212 atoms. This corresponds to the average molecular weight of the commercial Bakelite novolak given by Holland et al. [9] derived from gel permeation chromatography. Because recently performed MALDI measurements detected a distribution of about eight repeat units, two other ensembles were created: one ensemble consisted of chains with eight repeat units in ortho–ortho sequence, the second ensemble was made of chains of eight repeat units in 57% ortho–para and 43% in ortho–ortho sequence with respect to the methylene bridges to tailor the simulated structure more closely to the real sample

* Author to whom all correspondence should be addressed.

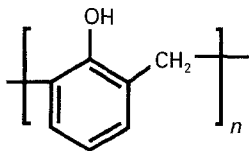


Figure 1 Repeat unit of formaldehyde phenol.

which has 50% ortho–para, 27% ortho–ortho and 23% para–para sequence according to NMR measurements in methanol. Each of the molecular chains was then energy minimized by the molecular mechanics and molecular dynamics method implemented in the Discover code [10] of Biosym Inc. Inter- and intramolecular interactions are described by the potential given in Equation 1

$$\begin{aligned}
 V = & \sum_r f_r (r - r_{eq})^2 + \sum_\alpha f_\alpha (\alpha - \alpha_{eq})^2 \\
 & + \sum_\Theta H_\Theta [1 + s \cos(n\Theta)] + \sum_\chi H_\chi \chi^2 \quad (1) \\
 & + \sum_{i < j} q_i q_j / \epsilon r_{ij} + \sum \epsilon [(r^*/r)^{12} - 2(r^*/r)^6]
 \end{aligned}$$

The force field parameters are taken from the pff force field of the Biosym polymer package [10]. Creation of the amorphous bulk state requires the single chain packed into a unit cell, which is infinitely repeated by periodic boundary conditions (p.b.c.) with an experimental density of 1.17 g cm^{-3} . In order to obtain reasonable statistics, ten molecules were packed into the p.b.c. box; during the packing procedure, the neighbourhood of each atom was checked by distance criteria: the sum of the van der Waals (vdW) radii must be the minimum distance between two non-bonded atoms. This structure is then prerelaxed by 1000 steps of conjugated gradient energy minimization using the full potential given in Equation 1 to remove bad contacts. In order to optimize the sample further, the system was subjected to annealing cycles of 20 ps duration where the temperature is decreased linearly from 1500 K to 300 K. After three cycles there was no further decrease of the potential energy. The same procedure was followed for the final temperatures $T = 450$ and 600 K. Because the density of the system for temperatures higher than room temperature is not known, the MD calculations at $T = 450$ and 600 K were performed for the NPT ensemble which previously incorporated the tail correction in order to remove the error in pressure due to the truncation of the nonbond (vdW) potential in the periodic cubic cell.

The MD simulations for the NPT ensemble are performed using the leap-frog algorithm with a time step of 1 fs. The temperature, T , is kept constant at 300, 450 and 600 K by the loose coupling algorithm of Berendsen *et al.* [11]. At each of these temperatures the MD runs were performed over 400 ps and frames of the trajectory were stored every 0.5 ps.

2.1. Analysis of the trajectories

The characteristic ratio

$$c_n = \frac{l}{nl^2} \langle r^2 \rangle_0 \quad (2)$$

is widely used as a measure of chain flexibility. In this expression, n is the number of chain segments, e.g. repeat units, l is the length of the chain segment and $\langle r^2 \rangle_0$ is the unperturbed square of the end-to-end distance. In our model, $l = 0.514 \text{ nm}$ and the chains consisted of 15 segments. The averaged end-to-end distance was $3.137 \pm 1.27 \text{ nm}$, the calculated characteristic ratio turns out to be 2.46, which indicates a coil-like structure. For the most flexible chains (e.g. Gaussian-like) one finds $c_n = 1.0$.

One way to characterize the amorphous structure of Novolak is to calculate the radial distribution function. We will present the total-, as well as the intra- and intermolecular radial distribution function. The function, $g_{ab}(r)$ gives the probability of finding atom b at a distance between r and $dr + r$ from atoms a as a function of the a – b separation, r , in the simulated structure

$$g_{ab}(r) = \frac{d\langle N_{ab}(r) \rangle}{\rho_{ab} dV(r)} \quad (3)$$

where $d\langle N_{ab}(r) \rangle$ is the average number of a – b pairs with a distance between r and $r + dr$, ρ_{ab} is the bulk density of type a and b atoms, and $d\langle N_{ab}(r) \rangle / dV(r)$ is the average local density of type a and b atoms in the shell volume $dV(r)$.

3. Local mode analysis

This method is suitable for calculating localized vibrations with high frequencies [12]. It assumes that fast vibrations can be treated separately from the slow intra- and intermolecular relaxations: the slow motions are modelled by a classical MD calculation and the fast motions are treated quantum mechanically. The MD trajectory contains a series of configurations in terms of cartesian coordinates and each of the configurations is frozen during a short vibrational time period. The local mode vibrations are considered as quantum oscillators in a mean field of surrounding atoms. The mean field

$$V^{\text{eff}}(Q) = K_0 + K_2 Q^2 + K_3 Q^3 + K_4 Q^4 \quad (4)$$

can be fitted to the local energy surface sampled by distorting the molecule along the vibrational modes. The frequencies are calculated by solving a one-dimensional Schrödinger equation on the effective potential

$$\frac{-\hbar^2}{2M} \left[\frac{d^2}{dQ^2} + V^{\text{eff}}(Q) \right] \Psi(Q) = E \Psi(Q) \quad (5)$$

The wavefunction is expanded in terms of eigenfunctions of the corresponding harmonic oscillator

$$\Psi(Q) = \sum_i C_i \phi_i(Q) \quad (6)$$

With this set of basis functions, the Schrödinger equation becomes a matrix eigenequation

$$HC = \varepsilon C \quad (7)$$

Diagonalization of the H -matrix gives energies of the ground state and several excited states, from which vibrational frequencies can be calculated. The following results were obtained by performing the procedure described above for 20 configurations extracted from trajectories of 2000 configurations stored every 100 fs and then accumulated in a histogram.

This vibrational analysis was performed on the basis of trajectories at 300, 450 and 600 K for the ensembles of ortho-para substituted chains. Our specific interest focused on the fast O-H vibration of these ensembles at different temperatures. The calculated frequencies for this vibration cover a region between 3350 and 3700 cm^{-1} . At a temperature of 300 K, the highest density of states appears at a frequency of about 3500 cm^{-1} and there are also four less-pronounced peaks: one at 3470 cm^{-1} and three peaks covering a region between 3540 and 3640 cm^{-1} . Increasing the temperature to 450 K reveals several peaks at higher frequencies (up to 3710 cm^{-1}) with low density of states compared to the main peak at approximately 3510 cm^{-1} . At 600 K, even more peaks of higher frequencies up to 3790 cm^{-1} occur. Temperature increase causes some of the OH "submolecules" to vibrate at frequencies $> 3550 \text{ cm}^{-1}$, which can be assigned to the frequency of a free O-H vibration. At the same time, the amount of bonded O-H vibrations, e.g. the density of states for the frequency region 3430–3570 cm^{-1} , decreases at the cost of the upcoming free O-H vibration.

Prior to any frequency analysis within our ensembles, we performed an *ab initio* creation of infrared spectra of novolak-type molecules. To obtain a clear impression of how infrared spectra evolve or change under the influence of different candidates for hydrogen-bonding in the typical frequency region of O-H bonds, we started out with theoretical calculations for 2,6-dimethylphenol followed by ortho-ortho-, ortho-para-, and para-para-novolak "dimers" (Fig. 2a–d). We performed energy minimization of these molecules *in vacuo* based on the pcff force field followed by molecular dynamics calculation storing the trajectory every 1 fs for a length of 10 ps. Then the dipole moment was calculated as a function of time. The Fourier transform of the dipole moment function gives the location of the corresponding infrared frequencies in the framework of the inherent approximations of the chosen method. For 2,6-dimethylphenol, the OH vibration covers a region between 3684 and 3729 cm^{-1} , which is very similar to that of the ortho-para novolak dimer. The OH vibration of the para-para novolak dimer shows a small shift to higher frequencies (3717–3737 cm^{-1}) which means that the OH vibration does not feel much of the interaction with the OH bond of the repeat unit in the para position. In the infrared spectrum of the ortho-ortho dimer we find a shift to lower frequencies (3600–3688 cm^{-1}) and a broadening of the peak shape caused by the close distance of the hydrogen and oxygen atoms of the two

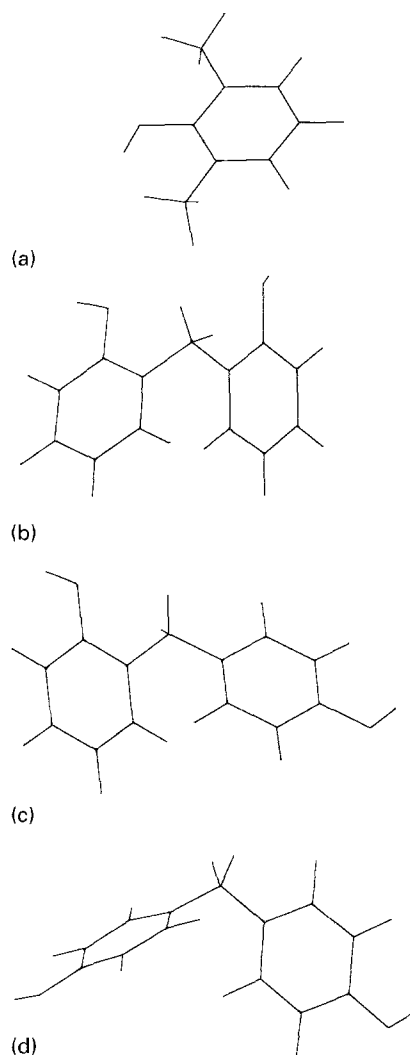


Figure 2 (a) 2,6-dimethylphenol, (b) ortho-dihydroxydiphenylmethane, (c) (ortho-hydroxyphenyl)(para-hydroxyphenyl)methane, (d) para-dihydroxydiphenylmethane.

different repeat units ($< 0.26 \text{ nm}$ on average). There is obviously the trend to a decrease in frequency when the perturbation of hydrogen bonding is switched on. (In any case, it is proved that a different atomistic environment has some effect on the calculated spectra. A similar result was obtained for the change of the infrared spectra of a water molecule and a water dimer. Additionally, the water test calculation shows that the pcff force field is capable of differentiating between hydrogen-bonded O-H stretching and non-bonded hydrogen stretching in the water dimer.) We also calculated the dipole moments of *bis(o-methylene)phenol* and the corresponding trimer by averaging over a 10 ps trajectory and obtained $\mu_{\text{Dim}} = \langle 2.96 \rangle$ Debye and $\mu_{\text{Trim}} = \langle 4.32 \rangle$ Debye. The experimental values [13] ($\mu_{\text{Dim}} = 2.46$ Debye and $\mu_{\text{Trim}} = 3.06$ Debye) are not directly comparable because they are measured in solution.

Another approach to tackle the problem of the distribution of free and hydrogen-bonded OH groups is to determine the radial distribution function (r.d.f.) of the total system, of the specific O...H group or of the O...O distances, respectively. The r.d.fs were calculated on the basis of the trajectories created for the ortho-para-substituted chains for three different

temperatures ($T = 300, 450$ and 600 K). The total r.d.f. for $T = 300$ K (Fig. 3) includes the distribution of all particles in the system and it demonstrates that there is only short-range order (up to 0.60 nm) which is due to the amorphous structure. The analysis of the trajectory with respect to the distribution of the oxygen atoms at 300 K led to the r.d.f. plotted in Fig. 4. Integration over $r = 0.26$ – 0.30 nm, which is the well-defined O...O distance of highly directional and short-range interaction of hydrogen bonding, gave a value of 9% , compared to the total integral of the O...O r.d.f. At a temperature of 600 K, the percentage of the oxygen atoms involved in hydrogen bonding decreases to a value of 6.7% . This effect is expected, but the amount of oxygen atoms involved in hydrogen bonding appears to be surprisingly small.

Analysis of the r.d.f. of the pure ortho–ortho ensemble with respect to the distance of oxygen atoms gives a value of 15.6% hydrogen-bonded oxygen atoms at 300 K. The correlation between a higher content of hydrogen bonds and a higher T_g value is well fulfilled: DSC measurement of the phenol formaldehyde resin with purely ortho linkages of the methylene groups leads to $T_g = 81$ °C [14] compared to $T_g = 57$ °C of our novolak resin. There still remains the

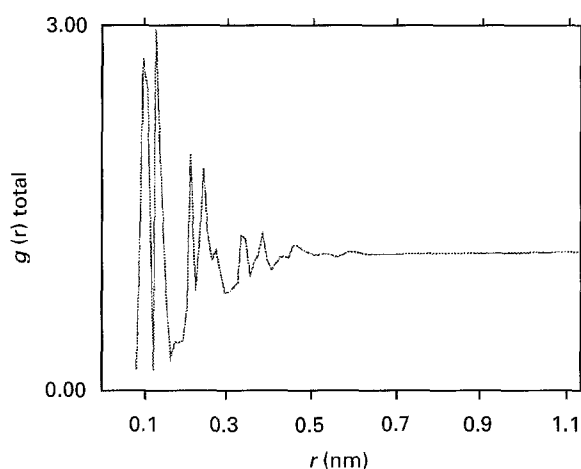


Figure 3 Total radial distribution function (r.d.f.) at 300 K averaged from a 300 ps trajectory for the ensemble consisting of differently substituted chains.

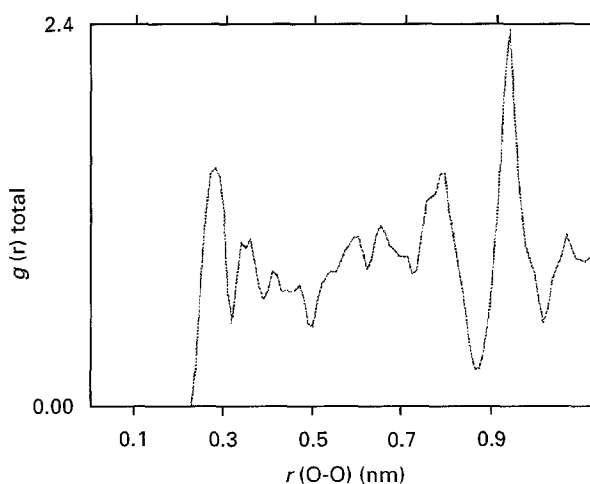


Figure 4 Radial distribution function (r.d.f.) at 300 K of all oxygen atoms in the ensemble of differently substituted chains.

question about the specific type of hydrogen bonds (intra- or intermolecular). To focus on this, the intra- and intermolecular radial distribution functions were calculated based on the trajectory of the pure ortho–ortho ensemble obtaining the result that 4.3% of the oxygen atoms are intermolecularly hydrogen bonded and 11.3% are intramolecularly hydrogen bonded.

4. Experimental infrared investigation with respect to hydrogen bonding

In principle, hydrogen bonding decreases the valence vibrational frequency, and it broadens the vibrational band, while, at the same time, the intensity of the band increases.

The use of the terms “free” and “associated” refers to the assignment already made in several papers [14,15]. Most of these publications deal with oligomers of differently substituted phenols in dilute solutions. In the highly dilute solute environment a sharp band at a frequency of 3610 cm^{-1} is detected and attributed to a free O–H stretching vibration. If the phenol concentration is increased, hydrogen bonds are created, being evident in a broad band about 3300 cm^{-1} .

The Novolak 1940H was not soluble in non-polar solvents. Therefore, a melting film was prepared on a silicon disc and heated up to 120 °C starting from room temperature using a non-commercial temperature cell which was implemented in a NICOLET 800 spectrometer. The spectra were recorded at intervals of 10° at a resolution of 4 cm^{-1} taking 64 scans.

Fig. 5 shows the infrared spectra of the Novolak 1940H in the hydroxyl stretching region from 3000 – 3650 cm^{-1} at different temperatures. At room temperature we observe the spectral region characteristic of two types of OH groups: a strong and broad band about 3380 cm^{-1} , which can be attributed to the class of associated OH groups, and a slightly less intense shoulder in the region between 3450 and 3580 cm^{-1} . According to the literature [6,7,15,16], there is evidence to assign this shoulder to “free” phenolic hydroxyls.

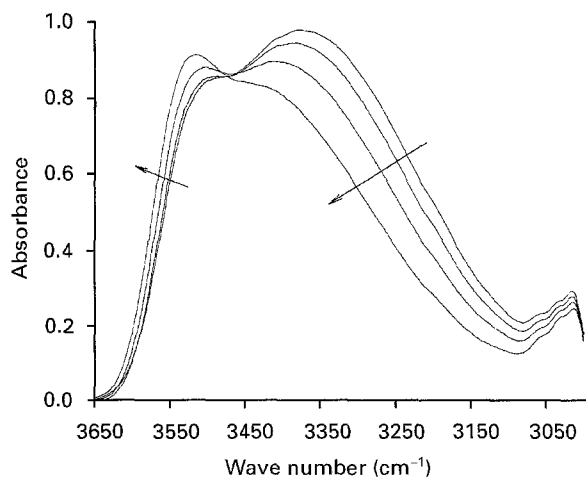


Figure 5 Spectra of Novolak 1940H in the OH stretching region at $30, 60, 90$ and 120 °C; temperature increase is indicated by the direction of the arrows.

Upon increasing the temperature from 30 °C to 120 °C, displayed in steps of 30 °C, we observe a change in the shape of the characteristic band in the O–H frequency region (Fig. 5): The shoulder attributed to the more or less “free” hydroxyls becomes more pronounced and intense at the cost of the band of the associated hydroxyls. At the temperature of 90 °C the two bands are best distinguishable; at 120 °C the “free” hydroxyl band is most intense.

Because it was not possible to obtain a reference measurement in non-polar solvents, we investigated PMMA/novolac mixtures. For these systems spectra were recorded at a resolution of 2 cm⁻¹. Samples were prepared for infrared analysis by casting a thin film on to a silicon disc from about 1% solutions of the two polymers in two different solvents. PMMA was dissolved in chloroform and Novolac in acetone.

Fig. 6a shows the infrared spectra for a 20:80 PMMA/novolac film in the hydroxyl stretching region from 3650–3000 cm⁻¹ (Fig. 6a) and in the carbonyl stretching region (Fig. 6b). For increasing temperature, the absorption of the shoulder in the OH stretching region grows and the intensity of the asso-

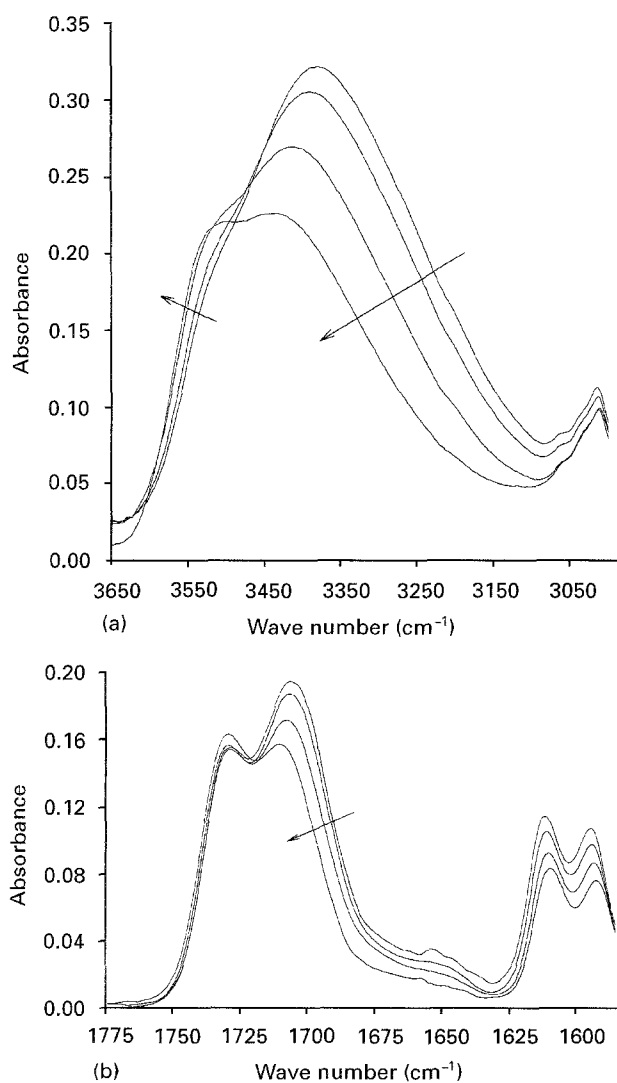


Figure 6 FT-IR spectra of PMMA/novolac (20:80 wt %) recorded to 30, 60, 90 and 120 °C; (a) in the OH stretching region and (b) in the carbonyl stretching region; temperature increase is indicated by the direction of the arrows.

ciated hydroxyls decreases, while the position of the maximum is changed to higher wave numbers. In the carbonyl region, there are two characteristic carbonyl group frequencies obtained by band separation (Table I): 1732 cm⁻¹ may be the contribution from the free carbonyl groups and 1706 cm⁻¹ can be attributed to the hydrogen-bonded carbonyl groups in analogy to the assignment made elsewhere [17]. The intensity ratio $v_{\text{ass}}/v_{\text{free}}$ decreases when temperature is raised from 30 °C to 120 °C, following the same trend observed in the hydroxyl stretching region of the pure novolac system: the area under the “free” carbonyl band increases, the area under the hydrogen-bonded carbonyl band decreases.

The infrared spectra recorded for thin films of PMMA/Novolak blends with contents of 20, 40, 60 and 80 wt % novolac show that the free hydroxyl is reduced with increasing PMMA content. A clearly visible shoulder is observed only in the case of 80 wt % novolac.

In Fig. 7 the carbonyl region of the infrared spectra of the different PMMA/novolac blends is displayed. With increasing novolac content the hydrogen-bonded CO absorption becomes stronger; at low novolac content only a little shoulder is found.

TABLE I Temperature dependence of the infrared spectra for the 20:80 PMMA/novolac blend

T (°C)	“Free” C=O band ν (cm ⁻¹)	Hydrogen-bonded C=O band	
		ν (cm ⁻¹)	Intensity ratio $v_{\text{ass}}/v_{\text{free}}$
30	1732	1706	1.63
60	1732	1706	1.56
90	1732	1708	1.34
120	1732	1709	1.18

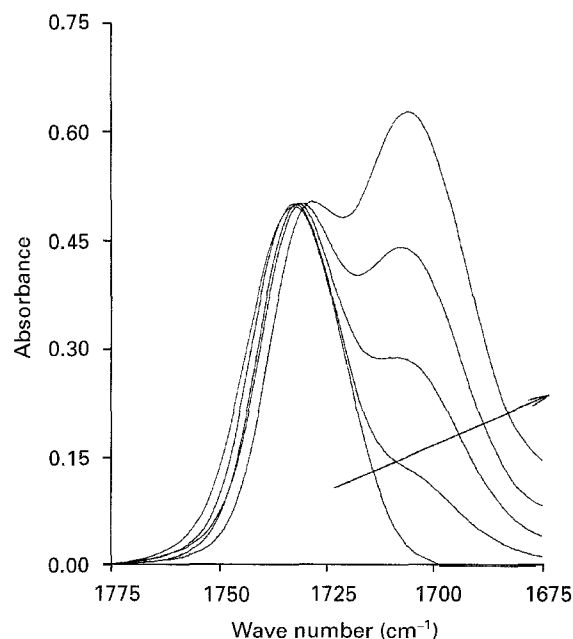


Figure 7 FT-IR spectra of PMMA/novolac blends in the carbonyl stretching region, recorded at room temperature, blends containing 0, 20, 40 and 80 wt % novolac; increasing content of novolac is indicated by the direction of the arrow. For a better overview, the intensity of the “free” carbonyl was set to absorbance = 0.5.

5. Conclusion

In this study we characterized the solid state of Novolak 1940 H mainly by analysis of trajectories obtained from atomistic computer simulation and infrared experiments. The latter investigation shows a qualitative effect of the broad bands assignable to "associated" and "free" O–H vibrations upon heating, which demonstrates that hydrogen bonding exists. Both experimental investigations (pure novolak and novolak/PMMA blend) can hardly be interpreted with respect to a quantitative amount of hydrogen bonding because the corresponding bands cannot be clearly resolved. The results obtained from computer simulation give a quantitative amount of hydrogen bonds within the novolak system which, when compared to the amount in the pure ortho-substituted system, is quite small. Nevertheless, it is easy to understand why hydrogen bonding in the pure ortho-substituted system is much more successful: the polar OH groups are a priori much closer to each other than in the differently substituted system. In both systems, it was found that hydrogen bonding mainly acts intramolecularly. Along the same lines, it is evident that a higher T_g value is correlated to the specific type of linkage within the molecular chains: the pure ortho substitution leads to a more favourable hydrogen bonding interaction and raises T_g .

Acknowledgement

We are indebted to Dr Krüger, ACA Adlershof, for carrying out the MALDI measurements, to Dr J. Kelm (BAM) for providing us with NMR spectra of

the novolak phenolic resin, and to Dr A. Reklat for performing the band separation.

References

1. D. N. THEODOROU and U. W. SUTER, *Macromolecules* **18** (1985) 1467.
2. *Idem, ibid.* **19** (1986) 139.
3. A. A. GUSEV, S. ARIZZI and U. W. SUTER, *J. Chem. Phys.* **99** (1993) 2221.
4. A. A. GUSEV and U. W. SUTER, *ibid.* **99** (1993) 2228.
5. G. L. BRODE, in "Encyclopedia of Chemical Technology", edited by Kirk-Othmer (Wiley, New York, 1982) pp. 384–416.
6. T. CAIRNS and G. EGLINGTON, *Nature* **196** (1962) 535.
7. *Idem, J. Chem. Soc.* (1965) 5906.
8. Z. KATOVIC and M. STEFANIC, *Ind. Eng. Chem. Prod. Res. Dev.* **24** (1985) 179.
9. C. HOLLAND, W. STARK and G. HINRICHSEN, *Acta Polym.* **46** (1995) 64.
10. Discover version 3.2, Biosym Technologies Inc., San Diego, CA (1994).
11. H. J. C. BERENDSEN, J. P. M. POSTMA, W. F. VAN GUNSTEREN, A. DINOLA and J. R. HAAK, *J. Chem. Phys.* **81** (1984) 3684.
12. H. SUN, R. O. WATTS and O. BUCK, *J. Chem. Phys.* **96** (1992) 1810.
13. F. L. JOBIASON, K. HOUGLUM and K. SHANAFELT, *ACS Polym. Preprints* **24** (1983) 181.
14. T. P. YOUNG, E. M. PEARCE, T. K. KWEI and N. L. YANG, *Macromolecules* **22** (1989) 1813.
15. G. SOCRATES, "Infrared Characteristic Group Frequencies" (Wiley, New York, 1980).
16. C. ZETTA, A. DE MARCO, G. CASIRAGHI, M. CORNIA and R. KAPTEIN, *Macromolecules* **18** (1985) 1095.
17. C. J. SERMAN, P. C. PAINTER and M. M. COLEMAN, *Polymer* **32** (1991) 1049.

Received 8 August

and accepted 15 December 1995